Self-Assembly of Binuclear Cu(II)-Histidine Complex for Absolute Configuration and Enantiomeric Excess Determination of Naproxen by Tandem Mass Spectrometry

Xiangying Yu,[a,b] Man-Chu Chau,[c] Wai Kit Tang,[c] Chi-Kit Siu,[c]* Zhong-Ping Yao[a,d,e]*

[a]State Key Laboratory of Chinese Medicine and Molecular Pharmacology (Incubation), Shenzhen Research Institute of Hong Kong Polytechnic University, Shenzhen 518057, China

[b]School of Chemical Engineering and Energy Technology, Dongguan University of Technology, Dongguan 523808, China

[c]Department of Chemistry, City University of Hong Kong, 83 Tat Chee Avenue, Kowloon Tong, Hong Kong SAR, China

[d]State Key Laboratory of Chirosciences, Food Safety and Technology Research Centre and Department of Applied Biology and Chemical Technology, The Hong Kong Polytechnic University, Hung Hom, Kowloon, Hong Kong SAR, China

[e]Key Laboratory of Natural Resources of Changbai Mountain and Functional Molecules (Yanbian University), Ministry of Education, Yanji 133002, Jilin, China

***Corresponding author:**

Chi-Kit Siu

Department of Chemistry, City University of Hong Kong, 83 Tat Chee Avenue, Kowloon Tong, Hong Kong SAR, China

Tel: +852 34422272; fax: +852 3442 0522, email address: chiksiu@cityu.edu.hk

Zhong-Ping Yao

Department of Applied Biology and Chemical Technology, The Hong Kong Polytechnic University, Hung Hom, Kowloon, Hong Kong SAR, China

Tel: +852 2358 7332; fax: +852 2358 1559, email address: zhongping.yao@polyu.edu.hk

Abstract

Naproxen is one of the most consumed non-steroidal anti-inflammatory drugs and marketed as S-naproxen since R-naproxen is hepatotoxic. In this study, chiral recognition of naproxen has been investigated by tandem mass spectrometry (MS/MS). Among all diastereomeric complexes formed between naproxen and the examined chiral selectors, including cyclodextrins (α/β/γ-CD), modified phenylalanines (*N*-acetyl-phenylalanine, *N*-t-butoxycarbonyl-phenylalanine, *N*-9-fluorenylmethyloxycarbonyl-phenylalanine), amino acids (Trp, Phe, Tyr, His), glucose, tartaric acid and vancomycin, a novel binuclear metal bound diastereomeric complexes $[(M(II))_2(S/R\text{-Naproxen})(L\text{-His})_2\text{-}3H]^+$ (M = Cu, Ni or Co with Cu being the best) could allow effective identification of the absolute configuration of naproxen and determination of its enantiomeric excess (ee) through MS/MS analysis. The key candidate structure of $[(Cu(II))_2(S/R\text{-Naproxen})(L\text{-His})_2\text{-}3H]^+$ has been revealed by means of collision-induced dissociation, ion mobility mass spectrometry and density functional theory calculations, indicating an interesting and unusual self-assembly compact geometry with the two Cu(II) ions bridged closely together (Cu-Cu distance is 3.04 Å) by the carboxylate groups of the two histidines. It was shown that the difference in dissociation efficiency between the two diastereomers was attributed to the interaction between the NH_2 bond of the amino group of one histidine and the naphthyl ring of naproxen. The present report is the first to observe and characterize the complex of $(Cu(II))_2(His)_2$ with aromatic acid, which could contribute to the chiral recognition of other chiral aromatic acids, design of catalysts based on binuclear copper bound complex, as well as the better understanding of metal ion complexation by His or His-containing ligands.

Introduction

Chirality has attracted much interest in many fields such as chemical, biological, pharmaceutical and environmental sciences. Because of the intrinsic chiral environment of living systems, which are built from a series of chiral molecules such as carbohydrate, protein and nucleic acid, individual enantiomeric forms of drugs may produce different therapeutic or adverse effects through different processes of adsorption, distribution, metabolism or excretion.[1] As a result, the development and marketing of optically pure drugs have been growing rapidly due to the superiority of single enantiomeric drugs to racemates in reduced dose, increased potency and improved safety profile.[2] Following the current FDA guidelines on the recommendation of systematic pharmacological and toxicological investigation for individual enantiomers, it is essential to develop efficient and reliable chiral analysis methods for development and quality control of chiral drugs and the accurate environmental risk assessment of chiral drugs.[3]

Naproxen, a chiral pharmaceutical compound with the structure of 2-arylpropionic acid (see Figure 1 for the structure), is one of the most consumed non-steroidal anti-inflammatory drugs (NSAIDs).[4] It possesses anti-inflammatory and analgesic activities by inhibiting cyclooxygenase enzymes (COX).[5] Naproxen is suggested to be the lowest risk NSAID[6] among many others that can cause cardiovascular complications resulting from the activity of COX inhibition.[7] It is reported that the therapeutic effect of NSAIDs is exerted almost exclusively by their S-enantiomer.[1] Unlike other two highly consumed NSAIDs, ibuprofen and ketoprofen, which are distributed as racemic mixtures, only the S-enantiomer of naproxen is marketed since

R-naproxen is hepatotoxic.[4] Development of efficient and reliable methods for chiral differentiation of naproxen is thus essential. As shown in Figure 1, the chiral carbon in naproxen is attached to naphthyl, carboxylic and methyl groups and a hydrogen atom. Because of the little activity for interactions and small difference for enantioselectivity[8] of the methyl group and hydrogen atom, chiral recognition of naproxen is difficult as comparing with other chiral molecules. Currently, chiral differentiation and quantification of naproxen enantiomers are mainly achieved by using traditional chromatographic methods, including chiral liquid chromatography and derivatization followed by liquid or gas chromatography.[4,5,9-11]

Because of the superiority in speed, sensitivity and specificity, mass spectrometry (MS) without chromatographic separation has attracted much interest in chiral recognition and quantification since the first report in 1977.[2,12,13] Since enantiomers show the same mass-to-charge ratio (*m/z*), chiral discrimination of enantiomers by MS relies on the introduction of a chiral selector (CS), which binds with the enantiomers covalently or non-covalently to form diastereomers. Based on the different behaviors of diastereomers in various MS techniques, such as their abundances in single-stage MS spectra,[14-16] dissociation efficiency in tandem mass spectrometry (MS/MS),[17-21] or drift time in ion-mobility mass spectrometry (IM-MS),[22,23] the discrimination of enantiomers could be achieved.

The MS-based chiral differentiation have been developed for many drugs, including DOPA, atenolol, ephedrine, pseudoephedrine, isoproterenol, norepinephrine, propranolol, flindokalner, etc.[24-30] However, to the best of our knowledge, there is no report on the chiral analysis of

naproxen using mass spectrometry. Since MS/MS analysis typically provides more reliable and consistent results than single-stage MS approach[31] and is applicable to different sorts of mass spectrometers,[32,33] MS/MS was used in this study to systematically explore the chiral discrimination of naproxen. Chiral selectors that are commonly used in MS/MS-based chiral analysis,[13] including cyclodextrins (α-CD, β-CD, γ-CD), modified amino acids (*N*-acetyl-phenylalanine (*N*-Ac-Phe), *N*-t-butoxycarbonyl-phenylalanine (*N*-Boc-Phe), *N*-9-fluorenylmethyloxycarbonyl-phenylalanine (*N*-Fmoc-Phe)), amino acids (L-Trp, L-Phe, L-Tyr, L-His), L-glucose and L-tartaric acid, as well as vancomycin that was used as the chiral selector for separation of naproxen enantiomers by capillary electrophoresis[34] and that allowed molecular recognition through CID of noncovalent complexes between vancomycin antibiotics and peptide ligand stereoisomers,[35] were chosen as the chiral selectors in this study. The emphasis was to explore the diastereomers achieving the chiral discrimination of naproxen as well as the origin of the chiral recognition through quantum chemical computational investigation. The present results revealed that the novel binuclear $[(Cu(II))_2(S/R\text{-}Naproxen)(L\text{-}His)_2\text{-}3H]^+$ complexes, featuring a self-assembly compact geometry with the two Cu(II) ions bridged closely together (Cu-Cu distance is 3.04 Å) by the carboxylate groups of the two histidines, outperformed other examined diastereomeric pairs for the chiral discrimination of naproxen.

Experimental

Materials

All optically pure chiral selectors (α-CD, β-CD, γ-CD, *N*-Ac-L-Phe, *N*-Boc-L-Phe, *N*-Fmoc-

L-Phe, L-Trp, L-Phe, L-Tyr, L-His, L-glucose, L-tartaric acid and vancomycin), copper chloride ($CuCl_2$), zinc chloride ($ZnCl_2$), nickel chloride ($NiCl_2$), cobalt chloride ($CoCl_2$), magnesium chloride ($MgCl_2$), sodium nitrate ($NaNO_3$), and R/S-naproxen were purchased from Aladdin (Shanghai, China) and used without further purification.

Chiral selectors and metal salts, $CuCl_2$, $ZnCl_2$, $NiCl_2$, $CoCl_2$, $MgCl_2$ and $NaNO_3$ were dissolved separately in water to achieve a concentration of 500 μM. Stock solutions of R- or S-naproxen at the concentration of 500 μM were prepared with 1:1 water/methanol. The sample solution used for MS analysis was prepared by mixing the stock solutions, and then diluting with 50:50 water:methanol (0.1% formic acid) or 100% methanol, to obtain a final solution containing 20 μM R- or S-Naproxen and 20 μM chiral selector. For detection of divalent metal ion adduct, a final solution containing 20 μM R/S-naproxen, 20 μM chiral selector and 10μM divalent metal ion ($CuCl_2$, $ZnCl_2$, $NiCl_2$, $CoCl_2$, $MgCl_2$) with 50:50 water:methanol as dilution solvent was prepared. For detection of multi-sodium adduct when using amino acid as selector, a final solution containing 20 μM R/S-naproxen, 20 μM amino acid and 20 μM $NaNO_3$ with100% methanol as dilution solvent was prepared.

Mass spectrometry

All experiments were performed using a Synapt G2 HDMS mass spectrometer (Waters, Manchester, UK). ESI conditions were as follows: capillary voltage, 3 kV; sampling cone, 30 V; extraction cone, 5 V; source temperature, 70-100 °C; desolvation temperature, 100-350 °C; cone gas, 50 L h^{-1}; desolvation gas, 500 L h^{-1}. All experiments were performed in the positive

ion mode. The sample solution was infused via the syringe pump at a flow rate of 5 μL min^{-1}. The complexes were confirmed through accurate monoisotopic masses, isotope patterns, and MS/MS results. All spectral data represented the combined fifty scans in the direct infusion experiments. For MS/MS analysis, the transfer collision energy was set to a value for which the abundance ratio of product ion to precursor ion was close to unity for one enantiomer of the analyte. For the traveling wave ion mobility (TWIM) experiments, the drift gas was N_2, the traveling wave height was set at 40 V, and four traveling wave velocities were chosen as 500, 550, 600 and 650 m s^{-1}. Considering that the well-studied polyalanines consisting of multi-alanine residues provide chemical characteristics resembling to the studied complexes with two histidine amino acids on the molecular surface, collision cross section (CCS) values of the investigated complexes were determined with singly protonated polyalanines as calibrants as described in the literature.[36] The concentration of the polyalanines solutions was 10 μg mL^{-1}.

Computational details

Structures of the most promising binuclear copper complexes of S/R-naproxen with L-His as the chiral selector were studied using density functional theory (DFT) at the unrestricted B3LYP level with a double-zeta 6-31++G(d,p) basis set. The key geometry was also examined using other functionals, including PBE0, M06 and ωB97X-D, with a larger triple-zeta 6-311++G(d,p) basis set. All geometry optimization and harmonic frequency analysis were performed using the Gaussian 09 program package.[37] Density functional theory-molecular dynamics (DFT-MD) simulations were carried out using the VASP program (Vienna Ab initio Simulation Package[38-41]). Perdew-Burke-Ernzerhof (PBE) generalized gradient approximation

was used for the exchange-correlation functional. Spin-polarized method was used. Optimized pseudopotentials for all atoms were constructed by means of the projector augmented wave (PAW) method. The electronic wave functions were described by a plane-wave basis set, with the cutoff energy being 283 eV. To reduce the interaction between the periodical images imposed by the plane-wave basis set, an ion was put in a cubic simulation box with a large dimension of 25 Å. The DFT-MD simulations on the Born-Oppenheimer potential-energy surface were performed by solving the Newtonian equations of motion with an integration time step of 0.5 fs at a constant temperature of 298 K controlled by a Nosé-Hoover thermostat. Theoretical collision cross sections were evaluated using the trajectory (TJ)[42] and the exact hard-sphere scattering (EHSS)[43] methods with the revised parameters.[44] The DFT-MD simulations for each studied complex were run for 10 – 20 ps. During an initial 5 ps, the average Ω_{theo} values had converged to below 1%. Therefore, the reported average Ω_{theo} values were obtained only with data beyond this initial 5-ps equilibration time.

Results and discussion

Formation and dissociation of diastereomers

Some chiral selectors (CS) with wide application in chiral analysis were chosen for chiral differentiation of naproxen (M). As summarized in Table 1, the formation of diastereomers depended on the chiral selector and solvent used. With cyclodextrins (β/γ-CD) as the selector, diastereomers $[Naproxen+\beta\text{-}CD+H]^+$ (including minor $[2Naproxen+2\beta\text{-}CD+2H]^{2+}$) (**1**) and $[Naproxen+2\gamma\text{-}CD+2H]^{2+}$ (**2**) could be detected only with 50:50 water:methanol (0.1 % formic

acid) as the solvent. When 100% methanol was used, only the sodium-bound selector could be detected. When modified phenylalanines, glucose and tartaric acid were used as the chiral selectors, sodium adduct trimers $[Naproxen+2CS+Na]^+$ (CS =*N*-Boc-Phe (**3**) or glucose (**7**)) could be detected with 100% methanol while the potassium adduct trimers $[Naproxen+2CS+K]^+$ (CS =*N*-Boc-Phe (**4**), *N*-Ac-Phe (**5**), glucose (**6**) or tartaric acid (**8**)) could only be detected with 50:50 water:methanol (0.1% formic acid). When the amino acids were used as the selectors, the multi-sodium adduct trimers $[Naproxen+2CS+4Na-3H]^+$ (CS = Tyr (**9**), Phe (**10**), His (**11**) and Trp (**14**)) could only be detected with 100% methanol; copper-bound diastereomers $[Cu(II)(Naproxen)(His)-H]^+$ (**12**) and $[(Cu(II))_2(Naproxen)(His)_2-3H]^+$ (**13**) could be detected with 50:50 water:methanol; copper-sodium bound diastereomer $[Cu(II)(Naproxen)(Trp)_2Na_2-3H]^+$ (**15**) could be detected when 50:50 water:methanol or 100% methanol were used with the latter resulting in a higher intensity. When α-CD, *N*-Fmoc-Phe or vancomycin was used as the selectors, no diasteromers containing the selector and naproxen were observed, which might be due to the smaller size of α-CD, large steric effect of *N*-Fmoc-Phe and lower interaction between naproxen and vancomycin. Generally, solvent of 50:50 water:methanol (0.1 % formic acid) was crucial for the detection of protonated complexes and potassium adduct complexes. Among the chiral selectors investigated, the copper-bound diastereomers $[Cu(II)(Naproxen)(His)-H]^+$ (**12**) and $[(Cu(II))_2(Naproxen)(His)_2-3H]^+$ (**13**) (Figure S1) were observed only with His as the chiral selector, which was likely because of the coordination site provided by the imidazole ring in the side chain of histidine in addition to its amino and carboxylic groups.[45,46]

Figure S2 in Supporting Information shows the collision-induced dissociation (CID) spectra of some typical naproxen-containing diastereomeric complex ions, including a) [Naproxen+2γ-CD+2H]$^+$ (**2**), b) [Naproxen+2*N*-Boc-Phe+Na]$^+$ (**3**), c) [Naproxen+2Glucose+K]$^+$ (**6**), d) [Naproxen+2Tartaric acid+K]$^+$ (**8**), e) [Cu(II)(Naproxen)(His)-H]$^+$ (**12**) and f) [Cu(II)(Naproxen)(Trp)$_2$Na$_2$-3H]$^+$ (**15**). For all except the copper-containing complexes, loss of naproxen was observed. Loss of selector was also observed for **6** and **8**, and for the latter the collision energy was set at 0 eV, indicating its loose intermolecular binding. Loss of CO_2 from [Cu(II)(Naproxen)(His)-H]$^+$ reflected that at least one carboxylic group was deprotonated and coordinated to Cu(II) in the structure.[47-51]

Chiral recognition of naproxen by MS/MS

The chiral recognition of naproxen in this work was examined by comparing the intensity ratio of product ion to precursor ionfor all detected diastereomeric ions. The chiral recognition ratio CR was defined as equation (1), meaning that the more different the CR value from unity, the higher degree of chiral recogntion.[52]

$$\mathrm{CR}_{\mathrm{R/S}} = \frac{r_{\mathrm{R-naproxen}}}{r_{\mathrm{S-naproxen}}} = \frac{\left(\dfrac{[\text{product ion}]}{[\text{precursor ion}]}\right)_{\mathrm{R-naproxen}}}{\left(\dfrac{[\text{product ion}]}{[\text{precursor ion}]}\right)_{\mathrm{S-naproxen}}}$$

or

$$\mathrm{CR}_{\mathrm{S/R}} = \frac{r_{\mathrm{S-naproxen}}}{r_{\mathrm{R-naproxen}}} = \frac{\left(\dfrac{[\text{product ion}]}{[\text{precursor ion}]}\right)_{\mathrm{S-naproxen}}}{\left(\dfrac{[\text{product ion}]}{[\text{precursor ion}]}\right)_{\mathrm{R-naproxen}}} \quad (1)$$

As shown in Table 1, no significant chiral discrimination was observed when β-CD, *N*-Ac-L-Phe, L-Glucose, L-Tyr, L-Phe and L-Trp were used as the chiral selectors. Enantioselectivity was obtained with γ-CD, *N*-Boc-L-Phe, L-Tartaric acid and L-His as the chiral selectors. Comparison of the results obtained with *N*-Ac-L-Phe and *N*-Boc-L-Phe suggested that the bulky Boc group improved the chiral discrimination. Interestingly, the most chiral discrimination of naproxen was obtained with $[(Cu(II))_2(Naproxen)(L\text{-}His)_2\text{-}3H]^+$ (**13**), which was dissociated almost solely to $[(Cu(II))_2(L\text{-}His)_2\text{-}CO_2\text{-}3H]^+$ (Figure 1a) with a $CR_{R/S}$ value of 0.856 ± 0.017. As shown in Figure S1, the relative intensity of $[(Cu(II))_2(Naproxen)(L\text{-}His)_2\text{-}3H]^+$ was ~5% (absolute intensity: $\sim 2\times10^3$ per scan), which was high enough for accurate chiral recognition. Similar chiral recognition pattern of naproxen with analog binuclear complexes of Ni(II) and Co(II) was also observed but with smaller enantioselectivity (Table S1), which was in agreement with a previous report that suggested better performance of copper ion over other ions.[18,53] Metal ions Mg(II) and Zn(II) were also investigated in this study, but with no binuclear metal bound complexes detected under our experimental conditions. Overall, the heterochiral complex (R-Naproxen, L-His) was more stable against dissociation than the homochiral complex (S-Naproxen, L-His) for all investigated binuclear metal bound complexes, which was also reported for metal bound trimers.[19,26,48,54,55] As shown in Figure 1a, D-His was also tested for chiral recognition of naproxen, with a $CR_{R/S}$ vaule of 1.146±0.042 obtained, confirming the chiral discrimination of His towards naproxen. Therefore, the absolute configuration of naproxen could be identified through the comparison between CID of $[(Cu(II))_2(Naproxen)(L\text{-}His)_2\text{-}3H]^+$ and $[(Cu(II))_2(Naproxen)(D\text{-}His)_2\text{-}3H]^+$. The same

configurations of His and naproxen (L/S or D/R) allow higher intensity ratio of product ion to precursor ion than the opposite configurations of His and naproxen (L/R or D/S).

The influence of anlayte concentration on the MS/MS-based enantioselectivity was also evaluated in this study. For the concentration ratios of 4:1, 2:1, 1:1, 1:2 and 1:3 between R-naproxen and L-His, intensity ratios of 1.287±0.035, 1.261±0.018, 1.262±0.037, 1.266±0.012 and 1.272±0.016 between product ion and precusor ion were obtained, respectively, indicating the negligile effect of analyte concentration on chiral analysis by the MS/MS method. This result was in agreement with the previous studies with MS/MS-based kinetic method[25,56] and chiral ratio method,[57] and demonstrated the reliability of the current method in the practical application of chiral analysis of naproxen.

Quantitative measurement of enantiomeric purities of naproxen

As shown in the Supporting Information, equation (2) could be obtained between *ee* and *r*, the ratio of $[(Cu(II))_2(L\text{-}His)_2\text{-}CO_2\text{-}3H]^+$ to $[(Cu(II))_2(Naproxen)(L\text{-}His)_2\text{-}3H]^+$, where r_0 is the *r* value of the racemic sample (i.e., $r_0 = a + b/c$), and a, b, and c are constants.

$$\frac{1}{r - r_0} = -\frac{c^2}{b} \cdot \frac{1}{ee} - \frac{c}{b} \qquad (2)$$

Thus, a calibration curve for *ee* determination can be achieved by plotting $1/(r\text{-}r_0)$ versus $1/ee$. Similar method was established for chiral analysis of amino acids by using the ratio between protonated dimeric product ion to protonated trimeric precursor ion as *r*.[58]

By measuring the *r* value of naproxen samples with different *ee* in dissociation analysis of $[(Cu(II))_2(L\text{-}His)_2\text{-}CO_2\text{-}3H]^+$ to $[(Cu(II))_2(Naproxen)(L\text{-}His)_2\text{-}3H]^+$, the linear relationship between $1/(r\text{-}r_0)$ versus $1/ee$ was obtained with a linear coefficient of 0.98772 (Figure 1b), providing a fast and sensitive quantitative chiral analysis of naproxen. A naproxen solution with "unknow" ee was analyzed by the present method, and determined to be -48.7%±1.84% ee. Compared with the true value of -50.0% ee, the absolute error was 1.3% ee. Based on the sample concentration (20 μM), flowrate (5 μL min^{-1}) and infusion time (2 min), it could be estimated that 200 pmole of naproxen sample was consumed for this analysis. According to our previous study on the concentration effect, similar results should be obtained with lower concentration (e.g., 5 μM) and thus lower amounts (e.g., 40 pmole) of the sample.

Origin of the chiral discrimination capability of $[(Cu(II))_2(Naproxen)(L\text{-}His)_2\text{-}3H]^+$

To better understand the fundamental molecular principle of the chiral discrimination capability of $[(Cu(II))_2(Naproxen)(L\text{-}His)_2\text{-}3H]^+$, their structures with S- and R-naproxen have been investigated in details by means of CID and ion mobility experiments as well as density functional theory simulations. CID experiments for $[(Cu(II))_2(Naproxen)(L\text{-}His)_2\text{-}3H]^+$ (*m/z* 663.06) at collision energy (CE) varying from 5 eV to 80 eV were conducted (Figure S3). Single dissociation channel was confirmed for CE up to 15 eV, giving $[(Cu(II))_2(L\text{-}His)\text{-}CO_2\text{-}3H]^+$ (*m/z* 388.96), which was still the most abundant product at a higher CE of 30 eV (Figure S4). At this high CE of 30 eV, some very low abundant product ions were also formed. Very interestingly, almost all these minor products contained Cu and His only (except $[(Cu(II))_2(Naproxen)(L\text{-}His)\text{-}CO_2\text{-}3H]^+$ (*m/z* 463.99), resulting from a loss of CO_2 from the

precursor). They were formed from loss of neutral molecules, such as naproxen, NH_3, CO_2, CO and H_2O. Surprisingly, both copper ions were retained in many of these products. Similar results were also observed at other collision energies studied (Figure S3). In addition, reduction of Cu(II) to Cu(I), which was commonly observed,[47] only became apparent at CE=30 eV and higher. All these observations strongly suggested that, in the precursor structures, naproxen was bound weaker than the two histidines and the two Cu(II) ions were probably tied together by the two stronger bound histidines.

Plausible structures for $[(Cu(II))_2(S\text{-Naproxen})(L\text{-His})_2\text{-}3H]^+$ with S-naproxen and two L-histidines were studied theoretically using DFT calculations at B3LYP/6-31++G(d,p) level. Initial geometries were constructed systematically based on several considerations, including the acidity of each functional group, the inter-ionic distance between the two cationic Cu(II) centers, the coordination geometry of the Cu(II) ions and the metal-ligand chelating ability. Intuitively, the three carboxylic groups might be deprotonated; the same doubly cationic charged Cu(II) centers would be separated apart; the d^9 electron configuration of Cu(II) would adopt a square planar geometry with one or two relatively weaker coordination(s) at the axial position resulting from the Jahn-Teller effect; and Cu(II) could strongly bind to the imidazole ring of histidine besides their amino and carboxylic groups[59] and also the carboxylic group of naproxen. Over 60 initial complex geometries containing S-naproxen and L-histidine were constructed and they were optimized to 33 distinct geometries, which could be grouped into six categories. The lowest energy geometry of each category is shown in Figure 2a (**1S**, **2S**, **3S**, **4S**, **5S**, **6S**). They were located at the triplet state. Singlet state calculations were also performed

for some selected geometries. In general, the triplet geometries were between 40 – 150 kJ mol^{-1} lying lower than the singlet ones when the two Cu(II) ions were close in space. For those geometries with two well-separated Cu(II) ions, their singlet states consisted of two antiparallel unpaired electrons (one in each Cu(II) ion) and they were almost isoenergetic to the triplet states. Therefore, only triplet states will be discussed in the following sections. Some optimized geometries as shown in Figure 2a were unexpected based on our original intuition. Interestingly, those surprising geometries indeed played the major role in the chiral discrimination of naproxen (see below).

As expected, all optimized geometries involved Cu(II) bindings with carboxylate anions, amino groups and imidazole rings. In the lower-lying **1S**, **2S**, **3S** and **4S**, all three carboxylic acid groups were deprotonated. Deprotonation at one or both amino group(s) resulted in the higher-lying **5S** and **6S**, respectively. The triplet spin densities were mainly shared at the two Cu centers separately (Figure S5), indicating that both of them were remained at the +2 oxidation state havingthe d^9 electron configuration. This was in agreement that, due to the Jahn-Teller effect, in most of the low-lying geometries both Cu(II) ions were either tetra-coordinated with an approximate square-planar geometry (Cu-X: 1.92 – 2.13 Å) or penta-coordinated with a square-planar base (Cu-X: 1.94 – 2.09 Å) and an elongated axial coordination (Cu-X: 2.11 – 2.59 Å).

Surprisingly, the Columbic repulsion between the two Cu(II) ions was not playing any significant role in the overall thermodynamics of the complex geometry. Only in **3S** and **4S**,

the two Cu(II) ions were well-separated by ligands with long internuclear distances of 5.76 Å and 6.87 Å, respectively. Much shorter internuclear distance was found in the lowest-energy geometry **1S** (3.04 Å). Similar results were also observed for **2S** (4.26 Å), **5S** (3.11 Å) and **6S** (2.76 Å). The Cu(II) ions in these geometries were bridged together by two carboxylate groups (**1S**), one carboxylate group (**2S**), one carboxylate group and one amido group (**5S**) and two amido groups (**6S**). For comparison, the closest Cu-Cu distance in crystalline CuO is 2.91 Å.[60] Despite the Columbic repulsion between the two Cu(II) ions, few analogous dinuclear organometallic Cu(II) complexes were also reported and their internuclear distances were around 2.95–3.03 Å as characterized by X-ray crystallography.[61-63] Thus, the present optimized geometries for the gas-phase $[(Cu(II))_2(S\text{-Naproxen})(L\text{-His})_2\text{-}3H]^+$ with short Cu-Cu distance are reasonable.

To better select and confirm the most plausible candidate geometry contributing to the chiral discrimination in the above MS/MS analysis, TWIM-MS experiments under N_2 as the drift gas and at a traveling wave height of 40 V with four different velocities (500, 550, 600, 650 m s^{-1}) were performed. The ion mobility spectra obtained under these conditions had no obvious difference. And the results for both diastereomeric complexes, $[(Cu(II))_2(S\text{-Naproxen})(L\text{-His})_2\text{-}3H]^+$ and $[(Cu(II))_2(R\text{-Naproxen})(L\text{-His})_2\text{-}3H]^+$, were essentially identical. To ease the interpretation of these TWIM-MS results, the collision cross section (CCS) of the complex was determined following the literature procedure[36] with singly protonated polyalanines as the calibrants of which CCS values measured under He as the drift gas are known.[64] Our calibrated

CCS of $[(Cu(II))_2(Naproxen)(L\text{-}His)_2\text{-}3H]^+$ (Ω_{expt}) is 154.8 $Å^2$ (with a standard deviation of 1.2 $Å^2$).

Theoretical CCS values (Ω_{theo}) of the B3LYP/6-31++G(d,p) optimized geometries were also evaluated using the trajectory (TJ) and exact hard-sphere scattering (EHSS) simulations with revised parameters.[44] As shown in Table 2, the two diastereomers of each geometry had similar Ω_{theo}, in agreement with the TWIM-MS experiments that they were indistinguishable. Ω_{theo} of **3S/R** and **4S/R** were significantly larger than Ω_{expt} by more than 10%, predicted by both TJ and EHSS models, because of the extended geometries imposed by the two well-separated Cu(II) ions. The other four geometries with shorter Cu-Cu interionic distances were more compact; among them, Ω_{theo} of **1S/R** and **2S/R** (TJ and EHSS) and **5S/R** (TJ) were deviated from Ω_{expt} within 3% only. The thermostability of all geometries (only for the diastereomers with S-naproxen) as shown in Figure 2a was further examined by means of DFT-MD simulations at a temperature of 298 K for at least 10 ps. The average Ω_{theo} values (and their standard deviations) computed using both TJ and EHSS models for the MD trajectories from 5 ps onward were summarized in Table 2. The average Ω_{theo} values of the much extended **3S** and **4S** were still more than 14% (TJ) and 17% (EHSS) larger than Ω_{expt}. **5S** and **6S** were also predicted to be 5%–11% larger than the experimental value. Very interestingly, the compact **2S** became a lot more extended under our MD conditions probably because the two Cu(II) ions in the optimized geometry were bridged by only one carboxylate group. Among all geometries studies, only **1S** was remaining sufficiently compact with the average Ω_{theo} deviated from Ω_{expt} by only 1.1 % (TJ) and 2.3 % (EHSS). Similar DFT-MD and CCS calculations for the analog

compact geometry of $[(Cu(II))_2(Aspirin)(L\text{-}His)_2\text{-}3H]^+$ gave Ω_{theo} of 139 $Å^2$ (TJ) and 140 $Å^2$ (EHSS), which were only -0.5% and 0.3 %, respectively, deviated from Ω_{expt} of 140 $Å^2$ (SD = 0.5 $Å^2$), further confirming the reliability of our proposed **1S** geometry (two Cu(II) ions bridged together by two oxygen from two carboxylate groups) for naproxen. For comparison, there is a Cu_2O_2 core present in the oxygenated form of tyrosinase (ligated by six histidine residues) with Cu-Cu distance of 3.5–3.6 Å.[65] Recently, three *Nτ*-imidazole bonded Cu_2O_2 species have also been synthesized successfully at solution temperature of -145 °C with Cu-Cu distance of approximately 3.6 Å.[66]

From the CCS analysis, it could be concluded that **1S/R** with the compact self-assembly binuclear geometry were the most plausible candidates responsible for the chiral discrimination of naproxen. As discussed above, this chiral discrimination was achieved based on the relative dissociation efficiency of the two diastereomers, equations (3) and (4), in the MS/MS analysis.

$$[(Cu(II))_2(S\text{-}Naproxen)(L\text{-}His)_2\text{-}3H]^+ \rightarrow [(Cu(II))_2(L\text{-}His)_2\text{-}CO_2\text{-}3H]^+ + S\text{-}Naproxen + CO_2 \quad (3)$$

$$[(Cu(II))_2(R\text{-}Naproxen)(L\text{-}His)_2\text{-}3H]^+ \rightarrow [(Cu(II))_2(L\text{-}His)_2\text{-}CO_2\text{-}3H]^+ + R\text{-}Naproxen + CO_2 \quad (4)$$

Since the product side of equations (3) and (4) are identical, the difference between their dissociation efficiencies should be qualitatively correlated with the relative energies of the precursor diastereomers. As summarized in Table 2, only for **1S** and **6S**, of which the free

energies were higher than those for **1R** and **6R**; in other words, the S-analogs would dissociate more effectively than the R-analogs. The results for the lowest-energy **1S/R** were further confirmed with other commonly used DFT functionals, including PBE0, M06 and ωB97X-D, with a larger triple-zeta 6-311++G(d,p) basis set; the relative free energy $\Delta G_{298}°$ of **1S** is consistently higher than that of **1R** for all functionals employed.

In both **1S** and **1R** (Figure 2b), a NH-π interaction between the amino group of a histidine and the naphthyl ring of naproxen was established. For **1R**, the NH bond was pointing almost perpendicularly toward a phenyl ring of the naphthyl group at an angle approximately of 96°. The distance between the amino nitrogen and the center of the interacted phenyl ring (N…aryl) was 4.05 Å. For **1S**, the geometry of this NH-π interaction was titled, with its angle reduced to approximately 64°, probably by the steric repulsion between the naphthyl ring and the methyl group of naproxen. And the N…aryl distance was increased to 4.34 Å. For comparison, the N…aryl distance in the benzene-NH_3 complex was determined to be 3.59 Å using microwave spectroscopy[67] and 3.6 Å using ab initio calculation at MP2/cc-pVTZ level,[68] which were closer to the analog distance in **1R**. Therefore, it is reasonable to conclude that **1S** being energetically higher, and hence dissociated more effectively, than **1R** is most likely attributed to its weaker NH-π interaction.

Conclusions

We have systematically investigated the chiral recognition of naproxen using several potential chiral selectors, including cyclodextrins, modified amino acids, amino acids, glucose, tartaric

acid and vancomycin, by means of tandem mass spectrometry (MS/MS). A novel complex $[(M(II))_2(S/R\text{-Naproxen})(L\text{-His})_2\text{-}3H]^+$ (M: Cu, Ni, Co) was observed for the first time, and the intensity ratio between product and precursor ions was successfully applied for the chiral differentiation of naproxen through the CID of $[(M(II))_2(S/R\text{-Naproxen})(L\text{-His})_2\text{-}3H]^+$ (M: Cu, Ni, Co) with Cu(II) performing the best. In general, the heterochiral complex was more stable against dissociation than the homochiral complex, providing an approach to detect the absolute configuration of naproxen. The linear calibration curve between $1/(r\text{-}r_0)$ and $1/ee$ allowed fast determination of *ee* for naproxen solutions. The lowest-energy structure of $[(Cu(II))_2(Naproxen)(L\text{-His})_2\text{-}3H]^+$ (**1S/R**) has been examined by means of CID, ion mobility mass spectrometry and density functional theories, revealing a compact self-assembly binuclear geometry with the two Cu(II) ions bridged closely together (Cu-Cu distance is 3.04 Å) by the carboxylate groups of the two histidines. In this lowest-energy geometry, a NH bond of the amino group of one histidine is interacting with the naphthyl ring. Such NH-π interaction is weaker in **1S** than in **1R** due to steric repulsion between the naphthyl ring and the methyl group in naproxen, and therefore the former is energetically higher and hence dissociated more effectively, allowing the capability of chiral discrimination of naproxen. In sum, this paper is the first to observe and characterize the novel self-assembly complex of $(Cu(II))_2(His)_2$ with aromatic acid, which could allow absolute configuration and enantiomeric excess determination of naproxen through MS/MS analysis. The established method can be applied with various mass spectrometers, and the novel complex may also be applied in the chiral recognition of other chiral aromatic acids, contributing to the design of catalysts based on binuclear copper bound complex, as well as the better understanding of metal ion complexation

by His or His-containing ligands.

Acknowledgements

This research was supported by Collaborative Research Fund of Hong Kong Research Grants Council (Grant No. C5031-14E), State Key Laboratory of Chirosciences, and The University Research Facility in Chemical and Environmental Analysis (UCEA) of The Hong Kong Polytechnic University. Chi-Kit Siu thanks Research Grants Council (Grant No. CityU 11300917) and City University of Hong Kong (CityU) (Grant No. 7004401) for financial supports. Wai Kit Tang acknowledges Chow Yei Ching School of Graduate Studies, CityU, for his postgraduate studentship and various outstanding academic performance scholarships. Man-Chu Chau thanks Department of Chemistry, CityU for awarding him a undergraduate research scholarship.

Supporting Information Available:

Derivation of the mathematical relationship between ee and r; Figures S1-S5; Tables S1-S2.

References

(1) Lin, G. Q.; You, Q. D.; Cheng, J. F. *Chiral drugs: chemistry and biological action*; Johh Widey & Sons, Inc.: Hoboken, New Jersey, 2011.

(2) Awad, H.; El-Aneed, A. *Mass Spectrom. Rev.* **2013**, *32*, 466-483.

(3) Camacho-Munoz, D.; Kasprzyk-Hordern, B. *Anal. Bioanal. Chem.* **2015**, *407*, 9085-9104.

(4) Caballo, C.; Sicilia, M. D.; Rubio, S. *Anal. Bioanal. Chem.* **2015**, *407*, 4721-4731.

(5) Hashim, N. H.; Khan, S. J. *J. Chromatogr. A* **2011**, *1218*, 4746-4754.

(6) McGettigan, P.; Henry, D. *PLoS Med.* **2013**, *10*, e1001388.

(7) Grosser, T.; Fries, S.; FitzGerald, G. A. *J. Clin. Invest.* **2006**, *116*, 4-15.

(8) Wu, L.; Vogt, F. G. *J. Pharm. Biomed. Anal.* **2012**, *69*, 133-147.

(9) Ogawa, S.; Tadokoro, H.; Sato, M.; Hanawa, T.; Higashi, T. *J. Chromatogr. B* **2013**, *940*, 7-14.

(10) Wang, L. L.; Deng, J.; Ji, X. Z.; Liu, W. B.; Liang, J.; Yan, X. N.; Chen, D.; Xie, J. *J. AOAC Int.* **2014**, *97*, 121-127.

(11) Shi, X. Y.; Liu, F. P.; Mao, J. Y. *Anal. Chim. Acta* **2016**, *912*, 156-162.

(12) Fales, H. M.; Wright, G. J. *J. Am. Chem. Soc.* **1977**, *99*, 2339-2340.

(13) Yu, X.; Yao, Z. *Anal. Chim. Acta* **2017**, *968*, 1-20.

(14) Bredikhina, Z. A.; Sharafutdinova, D. R.; Bazanova, O. B.; Babaev, V. M.; Fayzullin, R. R.; Rizvanov, I. K.; Bredikhin, A. A. *J. Inclusion Phenom. Macrocyclic Chem.* **2014**, *80*, 417-426.

(15) Seymour, J. L.; Tureček, F.; Malkov, A. V.; Kočovský, P. *J. Mass Spectrom.* **2004**, *39*, 1044-1052.

(16) Takai, Y.; Iguchi, K.; Yamada, H.; Shizuma, M.; Arakawa, R.; Sawada, M. *J. Mass Spectrom.* **2006**, *41*, 266-268.

(17) Berkecz, R.; Hyyrylainen, A. R. M.; Fulop, F.; Peter, A.; Janaky, T.; Vainiotalo, P.; Pakarinen, J. M. H. *J. Mass Spectrom.* **2010**, *45*, 1312-1319.

(18) Hyyrylainen, A. R. M.; Pakarinen, J. M. H.; Forro, E.; Fulop, F.; Vainiotalo, P. *J. Mass Spectrom.* **2010**, *45*, 198-204.

(19) Karthikraj, R.; Chitumalla, R. K.; Bhanuprakash, K.; Prabhakar, S.; Vairamani, M. *J. Mass Spectrom.* **2014**, *49*, 108-116.

(20) Fujihara, A.; Maeda, N.; Hayakawa, S. *J. Mass Spectrom.* **2015**, *50*, 451-453.

(21) Yao, Z. P.; Wan, T. S. M.; Kwong, K. P.; Che, C. T. *Chem. Commun.* **1999**, 2119-2120.

(22) Domalain, V.; Hubert-Roux, M.; Tognetti, V.; Joubert, L.; Lange, C. M.; Rouden, J.; Afonso, C. *Chem. Sci.* **2014**, *5*, 3234-3239.

(23) Yu, X.; Yao, Z. P. *Anal. Chim. Acta* **2017**, *981*, 62-70.

(24) Grigorean, G.; Lebrilla, C. B. *Anal. Chem.* **2001**, *73*, 1684-1691.

(25) Tao, W. A.; Gozzo, F. C.; Cooks, R. G. *Anal. Chem.* **2001**, *73*, 1692-1698.

(26) Tao, W. A.; Wu, L.; Cooks, R. G. *J. Med. Chem.* **2001**, *44*, 3541-3544.

(27) Augusti, D. V.; Augusti, R.; Carazza, F.; Cooks, R. G. *Chem. Commun.* **2002**, 2242-2243.

(28) Sivateela, T.; Nagaveni, V.; Prabhakar, S.; Vairamani, M. *Eur. J. Mass Spectrom.* **2011**, *17*, 177-186.

(29) Karthikraj, R.; Prabhakar, S.; Vairamani, M. *Rapid Commun. Mass Spectrom.* **2012**, *26*, 1385-1391.

(30) Wu, L. M.; Vogt, F. G.; Liu, D. Q. *Anal. Chem.* **2013**, *85*, 4869-4874.

(31) Tao, W. A.; Cooks, R. G. *Angew. Chem. Int. Ed.* **2001**, *40*, 757-760.

(32) Fago, G.; Filippi, A.; Giardini, A.; Laganà, A.; Paladini, A.; Speranza, M. *Angew. Chem. Int. Ed.* **2001**, *40*, 4051-4054.

(33) Wu, L. M.; Cooks, G. *Eur. J. Mass Spectrom.* **2005**, *11*, 231-242.

(34) Zhang, J. J.; Du, Y. X.; Zhang, Q.; Lei, Y. T. *Talanta* **2014**, *119*, 193-201.

(35) Jørgensen, T. J. D.; Delforge, D.; Remacle, J.; Bojesen, G.; Roepstorff, P. *Int. J. Mass Spectrom.* **1999**, *188*, 63-85.

(36) Smith, D. P.; Knapman, T. W.; Campuzano, I.; Malham, R. W.; Berryman, J. T.; Radford, S. E.; Ashcroft, A. E. *Eur. J. Mass Spectrom.* **2009**, *15*, 113-130.

(37) Frisch, M. J.; Trucks, G. W.; Schlegel, H. B.; Scuseria, G. E.; Robb, M. A.; Cheeseman, J. R.; Scalmani, G.; Barone, V.; Mennucci, B.; Petersson, G. A.; et al. *Gaussian 09*, revision D.01; Gaussian, Inc.: Wallingford, CT, 2013.

(38) Kresse, G.; Hafner, J. *Phys. Rev. B* **1993**, *47*, 558–561.

(39) Kresse, G.; Hafner, J. *Phys. Rev. B* **1994**, *49*, 14251–14269.

(40) Kresse, G.; Furthmuller, J. *Comput. Mater. Sci.* **1996**, *6*, 15-50.

(41) Kresse, G.; Furthmuller, J. *Phys. Rev. B* **1996**, *54*, 11169-11186.

(42) Mesleh, M. F.; Hunter, J. M.; Shvartsburg, A. A.; Schatz, G. C.; Jarrold, M. F. *J. Phys. Chem. C* **1996**, *100*, 16082-16086.

(43) Shvartsburg, A. A.; Jarrold, M. F. *Chem. Phys. Lett.* **1996**, *261*, 86-91.

(44) Siu, C.-K.; Guo, Y.; Saminathan, I. S.; Hopkinson, A. C.; Siu, K. W. M. *J. Phys. Chem. B* **2010**, *114*, 1204-1212.

(45) Ziegler, B. E.; Marta, R. A.; Burt, M. B.; McMahon, T. B. *Inorg. Chem.* **2014**, *53*, 2349-2351.

(46) Markovic, M.; Ramek, M.; Sabolovic, J. *Eur. J. Mass Spectrom.* **2014**, 198-212.

(47) Gatlin, C. L.; Turecek, F.; Vaisar, T. *J. Am. Chem. Soc.* **1995**, *117*, 3637-3638.

(48) Tao, W. A.; Zhang, D. X.; Nikolaev, E. N.; Cooks, R. G. *J. Am. Chem. Soc.* **2000**, *122*, 10598-10609.

(49) Wu, L. M.; Tao, W. A.; Cooks, R. G. *Anal. Bioanal. Chem.* **2002**, *373*, 618-627.

(50) Steill, J.; Zhao, J. F.; Siu, C. K.; Ke, Y. Y.; Verkerk, U. H.; Oomens, J.; Dunbar, R. C.; Hopkinson, A. C.; Siu, K. W. M. *Angew. Chem. Int. Ed.* **2008**, *47*, 9666-9668.

(51) Ke, Y.; Zhao, J.; Verkerk, U. H.; Hopkinson, A. C.; Siu, K. W. M. *J. Phys. Chem. B* **2007**, *111*, 14318-14328.

(52) Ravikumar, M.; Prabhakar, S.; Vairamani, M. *Chem. Commun.* **2007**, 392-394.

(53) Kumari, S.; Prabhakar, S.; Vairamani, M.; Devi, C. L.; Chaitanya, G. K.; Bhanuprakash, K. *J. Am. Soc. Mass Spectrom.* **2007**, *18*, 1516-1524.

(54) Zhang, D. X.; Tao, W. A.; Cooks, R. G. *Int. J. Mass Spectrom.* **2001**, *204*, 159-169.

(55) Kumari, S.; Prabhakar, S.; Vairamani, M. *Rapid Commun. Mass Spectrom.* **2008**, *22*, 1393-1398.

(56) Tao, W. A.; Wu, L. M.; Cooks, R. G. *Chem. Commun.* **2000**, 2023-2024.

(57) Yao, Z. P.; Wan, T. S. M.; Kwong, K. P.; Che, C. T. *Anal. Chem.* **2000**, *72*, 5383-5393.

(58) Yao, Z. P.; Wan, T. S. M.; Kwong, K. P.; Che, C. T. *Anal. Chem.* **2000**, *72*, 5394-5401.

(59) Dunbar, R. C.; Martens, J.; Berden, G.; Oomens, J. *Phys. Chem. Chem. Phys.* **2016**, *18*, 26923-26932.

(60) Åbrink, S.; Waskowska, A. *J. Phys.: Condens. Matter* **1991**, *3*, 8173-8180.

(61) Peng, Q. X.; Lin, C. N.; Zhang, Y. X.; Zhan, S. Z.; Ni, C. L. *Z. Anorg. Allg. Chem.* **2016**, *642*, 860-865.

(62) Nakajima, T.; Yamashiro, C.; Taya, M.; Kure, B.; Tanase, T. *Eur. J. Inorg. Chem.* **2016**, *2016*, 2764-2773.

(63) Colacio, E.; Perea-Buceta, J. E.; Mota, A. J.; Brechin, E. K.; Prescimone, A.; Hanninen, M.; Seppala, P.; Sillanpaa, R. *Chem. Commun.* **2012**, *48*, 805-807.

(64) Henderson, S. C.; Li, J.; Counterman, A. E.; Clemmer, D. E. *J. Phys. Chem. B* **1999**, *103*, 8780-8785.

(65) Matoba, Y.; Kumagai, T.; Yamamoto, A.; Yoshitsu, H.; Sugiyama, M. *J. Biol. Chem.* **2006**, *281*, 8981-8990.

(66) Chiang, L.; Keown, W.; Citek, C.; Wasinger, E. C.; Stack, T. D. P. *Angew. Chem. Int. Ed.* **2016**, *55*, 10453-10457.

(67) Rodham, D. A.; Suzuki, S.; Suenram, R. D.; Lovas, F. J.; Dasgupta, S.; Goddard III, W. A.; Blake, G. A. *Nature* **1993**, *362*, 735-737.

(68) Tsuzuki, S.; Honda, K.; Uchimaru, T.; Mikami, M.; Tanabe, K. *J. Am. Chem. Soc.* **2000**, *122*, 11450-11458.

Table 1. MS/MS results of the diastereomeric complex ions of naproxen (M) and various chiral selectors (CS).

Chiral selector (S)	Entry	Complex ion[a]	Product ion[b]	$r_{(R\text{-Naproxen})}$ $r_{(S\text{-Naproxen})}$	$CR_{R/S}$
β-CD	**1**	$[M+CS+H]^+$ *m/z* 1365.47 (A)	$[CS+H]^+$ *m/z* 1135.38 (8)	1.205±0.030 1.172±0.017	1.028±0.030
			$[M+2CS+2H]^{2+}$ *m/z* 1250.42 (8)	0.617±0.013 0.529±0.056	1.167±0.126
γ-CD	**2**	$[M+2CS+2H]^{2+}$ *m/z* 1412.48 (A)	$[2CS+2H]^{2+}$ *m/z* 1297.43 (8)	0.817±0.005 0.747±0.031	1.093± 0.046*
N-Boc-L-Phe	**3**	$[M+2CS+Na]^+$ *m/z* 783.35 (A, B)	$[2CS+Na]^+$ m/z 553.25 (4)	0.422±0.010 0.383±0.006	1.101±0.031*
	4	$[M+2S+K]^+$ *m/z* 799.32 (A)	$[2CS+K]^+$ *m/z* 569.23 (4)	0.540±0.004 0.520±0.005	1.038±0.013*
N-Ac-L-Phe	**5**	$[M+2CS+K]^+$ *m/z* 683.23 (A)	$[2CS+K]^+$ *m/z* 453.14 (3)	1.236±0.030 1.232±0.030	1.003±0.034
L-Glucose	**6**	$[M+2CS+K]^+$ *m/z* 629.18 (A)	$[2CS+K]^+$ *m/z* 399.09 (6)	0.235±0.013 0.249±0.006	0.945± 0.057
			$[M+CS+K]^+$ *m/z* 449.12 (6)	0.214±0.025 0.191±0.015	1.116 ±0.158
	7	$[M+2CS+Na]^+$ *m/z* 613.21 (B)	$[CS+Na]^+$ *m/z*203.05 (0)	NA[c] NA[c]	NA[c]
L-Tartaric acid	**8**	$[M+2CS+K]^+$ *m/z* 569.09 (A)	$[2CS+K]^+$ *m/z* 339.00 (0)	1.252±0.049 1.332±0.035	0.940±0.044
			$[M+CS+K]^+$ *m/z* 449.11 (0)	1.625±0.030 1.719±0.009	0.945±0.018*
L-Tyr	**9**	$[M+2CS+4Na-3H]^+$ *m/z* 681.18 (B)	$[2CS+4Na-3H]^+$ *m/z* 451.08 (18)	0.226±0.007 0.219±0.004	1.033±0.037
			$[CS+2Na-H]^+$ *m/z* 226.04 (18)	0.942±0.027 0.887±0.027	1.062±0.044
L-Phe	**10**	$[M+2CS+4Na-3H]^+$ *m/z* 649.18 (B)	$[M+CS+3Na-2H]^+$ *m/z* 462.13 (16)	0.223±0.004 0.230±0.005	0.968±0.027
			$[CS+2Na-H]^+$ *m/z* 210.05 (16)	0.700±0.019 0.699±0.006	1.001±0.028
L-His	**11**	$[M+2CS+4Na-3H]^+$ *m/z* 629.16 (B)	$[2CS+4Na-3H]^+$ *m/z* 399.07 (15)	1.337±0.109 1.316±0.077	1.015±0.102
			$[CS+2Na-H]^+$ *m/z* 200.04 (15)	0.756±0.034 0.741±0.023	1.021±0.056
	12	$[Cu(II)+M+CS-H]^+$ *m/z* 447.08 (C)	$[Cu(II)+M+CS-CO_2-H]^+$ *m/z* 403.10) (2.5)	0.342±0.004 0.321±0.002	1.067±0.014*
			$[Cu(I)+CS]^+$ *m/z* 217.99 (2.5)	0.849±0.012 0.889±0.008	0.955±0.016*
	13	$[2Cu(II)+M+2CS-3H]^+$ *m/z* 663.06 (C)	$[2Cu(II)+2CS-CO_2-3H]^+$ *m/z* 388.97 (8)	1.280±0.009 1.496±0.029	0.856±0.017**
L-Trp	**14**	$[M+2CS+4Na-3H]^+$ *m/z* 727.20 (B)	$[CS+2Na-H]^+$ *m/z* 249.06 (19)	1.020±0.117 1.027±0.013	0.994±0.114
	15	$[Cu(II)+M+2CS+2Na-3H]^+$ *m/z* 744.16(B, C)	$[CS+2Na-H]^+$ *m/z* 249.06 (18)	0.690±0.124 0.772±0.062	0.894±0.176

[a]Solvent used: (A) 50:50water:methanol (0.1% formic acid); (B) 100% methanol; (C) 50:50 water:methanol. [b]Collision energies (eV) used are shown in parentheses. [c]Intensity ratio was unavailable due to the very low intensity of the precursor ion even at the collision energy of 0 eV.*$p < 0.05$;**$p < 0.001$, by one-way ANOVA with Duncan's multiple range tests. The results given in the tables were means and standard deviations of at least three experiments.

Table 2. Results of relative energies at 0 K ($\Delta H_0°$ / kJ mol^{-1}) and free energies at 298 K ($\Delta G_{298}°$ / kJ mol^{-1}) of [(Cu(II))$_2$(S/R-Naproxen)(L-His)$_2$–3H]$^+$ as evaluated at B3LYP/6-31++G(d,p) level (unless stated otherwise), theoretical collision cross sections CCS (Ω_{theo} / Å^2) as evaluated using trajectory (TJ) and exact hard-sphere scattering (EHSS) simulations on the B3LYP/6-31++G(d,p) optimized geometries, and % Derivation as calculated using (Ω_{theo} - Ω_{expt})/Ω_{expt}×100%.

	Geometry optimization												**Molecular dynamics simulation**			
	Relative energy (kJ mol^{-1})				**Theoretical CCS (Ω_{theo} / Å^2)**				**%Derivation**				**Theoretical CCS (Ω_{theo} / Å^2)**		**%Derivation**	
	S		R		S		R		S		R					
	$\Delta H_0°$	$\Delta G_{298}°$	$\Delta H_0°$	$\Delta G_{298}°$	TJ	EHSS	TJ	EHSS	TJ	EHSS	TJ	EHSS	TJ (S.D.)	EHSS (S.D.)	TJ	EHSS
6	90.8	85.5	89.1	83.6	160.1	162.6	161.8	164.6	3.4	5.0	4.5	6.3	166.7 (3.0)	170.8 (3.2)	7.7	10.3
5	76.3	65.4	74.8	67.1	158.8	162.1	157.8	160.7	**2.6**	4.7	**1.9**	3.8	163.8 (4.2)	166.7 (4.5)	5.8	7.7
4	69.5	47.9	69.6	48.2	177.5	182.1	177.4	181.9	14.6	17.6	14.6	17.5	177.7 (2.7)	182.0 (2.4)	14.8	17.6
3	59.9	43.8	62.6	46.5	173.3	178.0	172.9	177.3	12.0	15.0	11.7	14.5	177.2 (2.3)	181.4 (2.2)	14.5	17.2
2	41.5	32.7	43.7	34.1	152.6	153.3	151.8	152.7	**-1.4**	**-1.0**	**-1.9**	**-1.4**	170.2 (3.3)	173.5 (3.1)	10.0	12.1
1	0.0	0.0	-0.5	-2.5	155.0	156.6	152.5	154.6	**0.1**	**1.2**	**-1.5**	**-0.2**	**156.4 (2.4)**	**158.3 (2.1)**	**1.1**	**2.3**
1[a]	0.0	0.0	-0.3	-3.1												
1[b]	0.0	0.0	-2.9	-2.8												
1[c]	0.0	0.0	-4.6	-4.4												
1[d]	0.0	0.0	-4.4	-6.5												

[a] B3LYP/6-311++G(d,p)

[b] PBE0/6-311++G(d,p)

[c] M06/6-311++G(d,p)

[d] ωB97X-D/6-311++G(d,p)

Figure captions

Figure 1. a) MS/MS spectra of $[(Cu(II))_2(R/S\text{-Naproxen})(L/D\text{-His})_2\text{-}3H]^+$ (monoisotopic *m/z* 663.06). The product ion of *m/z* 388.97 was identified as $[(Cu(II))_2(L/D\text{-His})_2\text{-}CO_2\text{-}3H]^+$ through the isotopic pattern and accurate masses. The collision energy of 8 eV in transfer cell was chosen. b) Plot of $1/(r\text{-}r_0)$ value as a function of 1/*ee*. Inset is the structure of naproxen.

Figure 2. a) Geometries of $[(Cu(II))_2(S\text{-Naproxen})(L\text{-His})_2\text{–}3H]^+$ optimized at the B3LYP/6-31++G(d,p) level. Relative energies at 0 K, $\Delta H_0°$, are in kJ mol^{-1}. b) The side-view of **1S** and **1R** optimized at B3LYP/6-31++G(d,p) level.

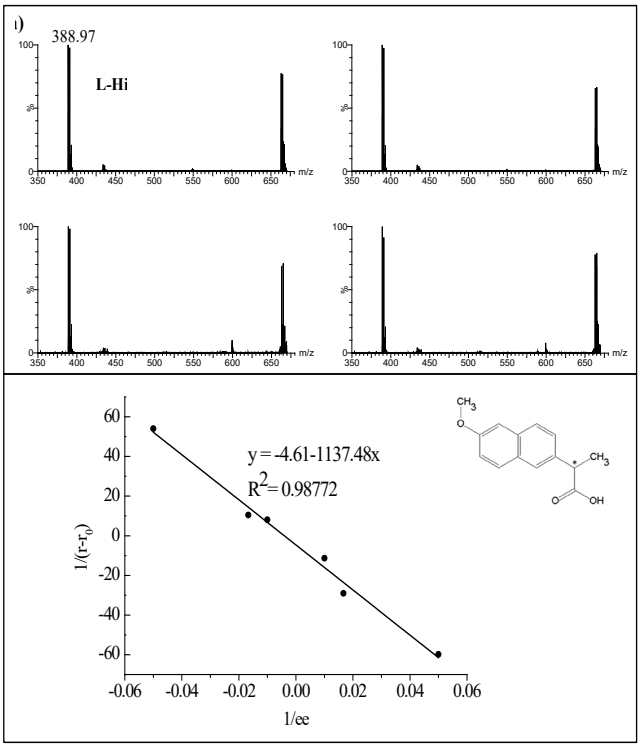

Figure 1

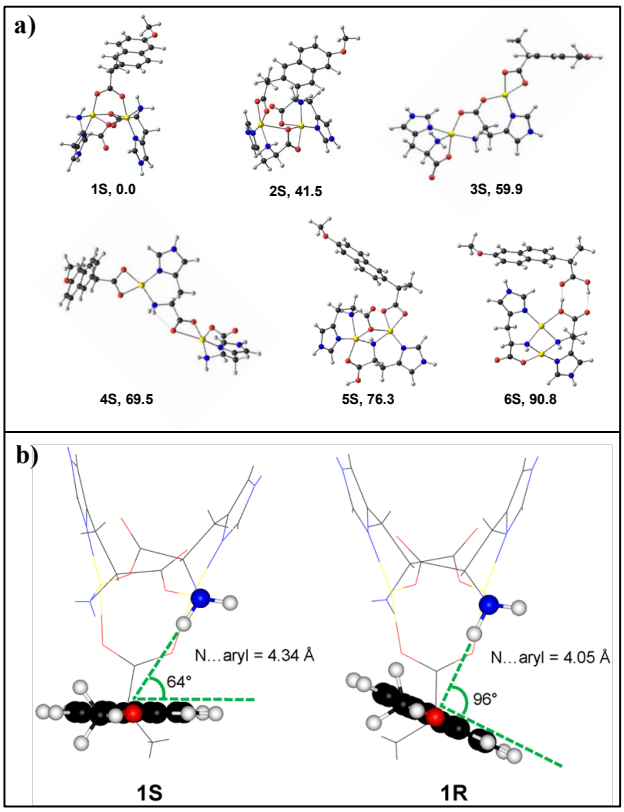
a)
1S, 0.0
2S, 41.5
3S, 59.9
4S, 69.5
5S, 76.3
6S, 90.8
b)
N…aryl = 4.34 Å
64°
N…aryl = 4.05 Å
96°
1S
1R

Figure 2

TOC only

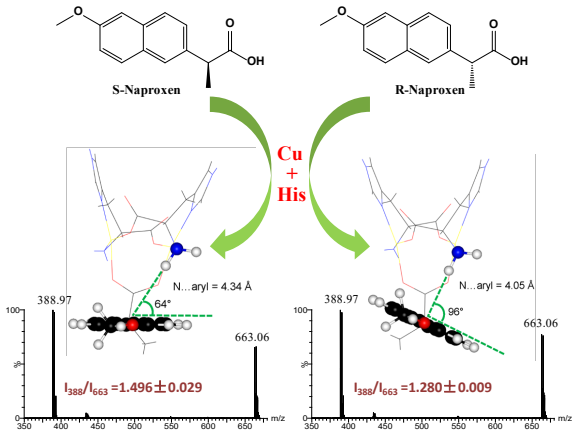
S-Naproxen
R-Naproxen
Cu
+
His
N...aryl = 4.34 Å
64°
388.97
663.06
I388/I663 =1.496±0.029
N...aryl = 4.05 Å
96°
388.97
663.06
I388/I663 =1.280±0.009